Advances and limitations of the Environmental Seismic Intensity scale (ESI 2007) regarding near-field and far-field effects from recent earthquakes in Greece: implications for the seismic hazard assessment

Q1 I. D. PAPANIKOLAOU[1,2]*, D. I. PAPANIKOLAOU[2] & E. L. LEKKAS[2]

[1]*Benfield-UCL Hazard Research Centre, Department of Earth Sciences, University College London, Gower Street, WC1E 6BT London, UK*

[2]*Natural Hazards Laboratory, Department of Dynamic, Tectonic and Applied Geology, Faculty of Geology and Geoenvironment, National and Kapodistrian University of Athens, Panepistimioupolis Zografou, 157-84 Athens, Greece*

**Corresponding author (e-mail: i.papanikolaou@ucl.ac.uk)*

Abstract: The new Environmental Seismic Intensity scale (ESI 2007), introduced by INQUA, incorporates the advances and achievements of palaeoseismology and earthquake geology and evaluates earthquake size and epicentre solely from the earthquake environmental effects (EEE). This scale is tested and compared with traditional existing scales for the 1981 Alkyonides earthquake sequence in the Corinth Gulf (Ms = 6.7, Ms = 6.4, Ms = 6.3), the 1993 Pyrgos event (Ms = 5.5) and the 2006 Kythira event (Mw = 6.7). These earthquakes were of different magnitudes, focal mechanisms and focal depths and produced well-documented environmental effects. The ESI 2007 intensity values and the isoseismal pattern for the 1993 Pyrgos and the 2006 Kythira events are similar to those resulting from the traditional scales, demonstrating that for moderate intensity levels (VII and VIII) the ESI 2007 and the traditional scales comply well. In contrast, the 1981 Alkyonides earthquake sequence shows that there is an inconsistency between the ESI 2007 and the traditional scales both in the epicentral area, where higher ESI 2007 intensity values have been assigned, and for the far-field effects. The ESI 2007 scale offers higher objectivity in the process of assessing macroseismic intensities, particularly in the epicentral area, than traditional intensity scales that are influenced by human parameters. The ESI 2007 scale follows the same criteria–environmental effects for all events and can compare not only events from different settings, but also contemporary and future earthquakes with historical events. A reappraisal of historical earthquakes so as to constrain the ESI 2007 scale may prove beneficial for seismic hazard assessment by reducing the uncertainty implied in the attenuation laws, which constitute one of the most important seismic hazard parameters.

A macroseismic intensity value represents the macroseismic information obtained by the quantification of the effects and damage produced by an earthquake. The macroseismic intensity is not solely used for the description of earthquake effects, but is a major seismic hazard parameter as well. The use of macroseismic intensity as a seismic hazard parameter predominates internationally, and more than 60% of countries have hazard assessment exclusively expressed in terms of intensity (McGuire 1993). The reason is that the historical record and the attenuation laws for large earthquakes are usually expressed in intensity values (e.g. Grandori *et al.* 1991), whereas in case of seismic risk management and earthquake loss estimation seismic intensity is preferred due to its direct representation of earthquake damage (Coburn & Spence 2002).

However, when using the effects on man and the manmade environment to assess the macroseismic intensity, then intensity will tend to reflect mainly the economic development and the cultural setting of the area that experienced the earthquake, instead of its ‘strength’ (Serva 1994). This led to the development and implementation of the Environmental Seismic Intensity 2007 scale. The newly introduced ESI 2007 scale (Michetti *et al.* 2007) is developed within the INQUA Subcommission on Palaeoseismicity, is the result of the revisions of previous versions, provisionally named as INQUA EEE scale (e.g. Michetti *et al.* 2004) and aims at evaluating earthquake size and epicentre solely from the earthquake environmental effects (EEE). The EEE are not influenced by human parameters such as effects on people and the manmade environment as the traditional intensity

From: REICHERTER, K., MICHETTI, A. M. & SILVA, P. G. (eds) *Palaeoseismology: Historical and Prehistorical Records of Earthquake Ground Effects for Seismic Hazard Assessment*. The Geological Society, London, Special Publications, **316**, 11–30. DOI: 10.1144/SP316.2 0305-8719/09/$15.00

scales (MCS, MM, EMS 1992, etc.) predominantly imply. It is a common notion that two earthquakes that produce similar environmental effects, thus having the same ESI 2007 intensity degree, but occur on sites that are different in terms of cultural and economic development, usually record significantly different intensity values as far as the traditional scales are concerned. In particular, if one of these earthquakes occurs in a developing country it tends to record a higher macroseismic intensity value compared to a developed seismic-prone country.

Over the last few decades palaeoseismology and earthquake geology have contributed significantly to our understanding concerning the EEE and more importantly they have provided a quantitative analysis and description of these effects. These effects have been incorporated into the ESI 2007 scale (Table 1). Among other advantages this scale: (i) allows the accurate assessment of intensity in sparsely populated areas, (ii) provides a reliable estimation of earthquake size with increasing accuracy towards the highest levels of the scale, where traditional scales saturate and ground effects are the only ones that permit a reliable estimation of earthquake size, and (iii) allows comparison among future, recent and historical earthquakes (Michetti *et al.* 2004). Overall, this scale is intended to integrate existing scales, not to replace them, and can encourage greater objectivity in the process of seismic intensity assessment, through independence from the variable nature of man and his infrastructure (Michetti *et al.* 2004). The use of the ESI 2007 scale alone is recommended only when effects on humans and manmade structures: (i) are absent or too scarce (i.e. desert or sparsely populated areas), and (ii) saturate (i.e. for intensity X to XII) losing their diagnostic value (Michetti *et al.* 2007).

Although the traditional intensity scales consider environmental effects for the evaluation of seismic intensity, these effects are not properly weighted and are systematically neglected. For example, the traditional scales do not differentiate between primary and secondary effects and do not use a quantitative approach for the effects on nature (Michetti *et al.* 2007). This is nicely illustrated with the EMS 1992 (European Macroseismic Scale) that forms an updated version of the traditional intensity scales (predominantly the MSK). The EMS 1992 was developed to be more easily implemented in urban areas giving even more emphasis to manmade structures. In particular, it includes new building types and modern construction materials, offers an easier recognition of the structure vulnerability class and a more precise evaluation of the grade of damage (Grunthal 1993).

In this paper we: (a) assess intensities in the ESI 2007 scale for several sites regarding three relatively recent events that occurred in Greece, (b) test and compare the ESI 2007 scale with existing traditional macroseismic intensity scales, and (c) discuss possible implications for seismic hazard assessment. The success of the newly introduced intensity scale also depends on its impact on seismic hazard assessment.

Selected earthquakes

An earthquake sequence and two events have been chosen for our current study (Fig. 1). These include the 1981 Alkyonides earthquake sequence in the Corinth Gulf (Ms = 6.7, Ms = 6.4, Ms = 6.3), the 1993 Pyrgos event (Ms = 5.5) and the 2006 Kythira event (Mw = 6.7). These earthquakes have been carefully selected so as to include events of different magnitudes, focal mechanisms and focal depths. Moreover, they all produced well documented environmental effects that allow us both to test the newly introduced ESI 2007 scale and compare it with the existing scales. In particular, the 1981 Alkyonides earthquake sequence produced significant primary surface ruptures, the 1993 Pyrgos event was on the threshold of primary faulting, producing only secondary but widespread effects, whereas the 2006 Kythira earthquake was a deep event that generated only minor secondary effects.

The 1993 Pyrgos earthquake

The 26 March 1993 Pyrgos (Ms = 5.5) earthquake in the Western Peloponnese produced a maximum intensity VIII on the EMS 1992 scale (Lekkas 1996), affecting the town of Pyrgos, where about 50% of the buildings suffered some form of damage (Figs 2 and 3a). The main shock of Ms = 5.5 occurred about 3 km south of the town of Pyrgos (Stavrakakis 1996). Two foreshocks of Ms = 5.0 (in the offshore area with thrust faulting) and Ms = 5.1 (normal faulting NE–SW plane dipping southwards) occurred 13 and 2 minutes before the main shock (Stavrakakis 1996). Papanastassiou *et al.* (1994) determined that the fault plane solution is characterized by thrust oblique faulting on a fault plane striking NNE–SSW and dipping SE (strike 14° dip 70° rake 158°), which according to Stavrakakis (1996) best fits the observed macroseismic field. A similar solution has been proposed by Dziewonski *et al.* (1994) (NP1 strike 122°, dip 60°, rake 5°, and NP2 strike 30°, dip 86°, rake 150°) and Melis *et al.* (1994). However, Koukouvelas *et al.* (1996) proposed that the Pyrgos earthquake was caused by oblique-normal slip on a north-dipping WNW-trending fault. Indeed, most outcropping active faults in the area are normal east–west trending faults (e.g. Lekkas *et al.* 2000;

Table 1. *Summary of the Environmental Seismic Intensity scale (ESI 2007) for intensities VII–X (Michetti* et al. *2007)*

EEE type/degree	VII Damaging – Appreciable effects on the environment	VIII Heavily damaging – Extensive effects on the environment	IX Destructive – Environmental effects are a widespread source of considerable hazard and become important for intensity assessment	X Very destructive – Effects in the environment become a leading source of hazards and are critical for intensity assessment
Surface faulting	Primary effects observed very rarely.	Primary effects observed rarely. Ground ruptures (surface faulting) may develop, up to several hundred meters long, with offsets not exceeding a few cm, particularly for very shallow focus earthquakes. Tectonic subsidence or uplift with maximum values on the order of a few centimetres may occur.	Primary effects observed commonly. Ground ruptures (surface faulting) develop, up to a few km long, with offsets generally in the order of several cm. Tectonic subsidence or uplift of the ground surface with maximum values in the order of a few decimetres may occur.	Primary ruptures become leading. Surface faulting can extend for few tens of km, with offsets from tens of cm up to a few metres. Gravity grabens and elongated depressions develop; Tectonic subsidence or uplift with maximum values in the order of few meters may occur.
Slope movements	Scattered landslides occur in prone areas; (steep slopes of loose/saturated soils; rock falls on steep gorges, coastal cliffs) their size is sometimes significant (10^3–10^5 m^3. The affected area is in the order of 10 km^2.	Small to moderate (10^3–10^5 m^3) landslides widespread in prone areas; their size is sometimes large (10^5–10^6 m^3). Ruptures, slides and falls affect riverbanks and artificial embankments in loose sediment or weathered/ fractured rock. The affected area is in the order of 100 km^2.	Landsliding widespread in prone areas, also on gentle slopes; where equilibrium is unstable (steep slopes of loose/saturated soils; rock falls on steep gorges, coastal cliffs) their size is frequently large (10^5 m^3), sometimes very large (10^6 m^3). Riverbanks, artificial embankments and excavations (e.g. road cuts, quarries) frequently collapse. The affected area is in the order of 1000 km^2.	Large landslides and rock-falls ($>10^5$–10^6 m^3) are frequent, practically regardless of equilibrium state of the slopes, causing temporary or permanent barrier lakes. River banks, artificial embankments, and sides of excavations typically collapse. Levees and earth dams may even incur serious damage. The affected area is in the order of 5000 km^2.

(*Continued*)

Table 1. *Continued*

EEE type/degree	VII Damaging – Appreciable effects on the environment	VIII Heavily damaging – Extensive effects on the environment	IX Destructive – Environmental effects are a widespread source of considerable hazard and become important for intensity assessment	X Very destructive – Effects in the environment become a leading source of hazards and are critical for intensity assessment
Ground cracks	Fractures up to 5–10 cm wide and up to hundred metres long commonly in loose alluvial deposits and/or saturated soils; Centimetre-wide cracks common in paved (asphalt or stone) roads.	Fractures up to 50 cm wide and up to hundred metres long are commonly observed in loose alluvial deposits and/or saturated soils; in rare cases fractures up to 1 cm can be observed in competent dry rocks. Decimetric cracks common in paved roads, as well as small pressure undulations.	Fractures up to 100 cm wide and up to hundred metres long are commonly observed in loose alluvial deposits and/or saturated soils; in competent rocks they can reach up to 10 cm. Significant cracks common in paved (asphalt or stone) roads, as well as small pressure undulations.	Open ground cracks up to more than 1 m wide and up to hundred metres long are frequent, mainly in loose alluvial deposits and/or saturated soils; in competent rocks opening reaches several decimetres. Wide cracks develop in paved (asphalt or stone) roads, as well as pressure undulations.
Ground settlements–collapse/tsunami/other effects	Rare cases of liquefaction, with sand boils up to 50 cm in diameter, in areas most prone to this phenomenon (highly susceptible, recent, alluvial and coastal deposits, shallow water table).	Liquefaction may be frequent in the epicentral area; sand boils up to *c.* 1 m in diameter; localized lateral spreading and settlements (subsidence up to *c.* 30 cm), with fissuring parallel to waterfront areas (river banks, lakes, canals, seashores). Waves up to 1–2 m high develop in nearshore areas and may damage of wash away objects of variable size.	Liquefaction and water upsurge are frequent; sand boils up to 3 m in diameter; frequent lateral spreading and settlements (subsidence of more than *c.* 30 cm), with fissuring parallel to waterfront areas (river banks, lakes, canals, seashores). Metre-high waves develop in still and running waters. Tsunamis may reach the coastal areas with runups of up to several metres flooding wide areas. Small boulders and tree trunks may be thrown in the air.	Liquefaction, with water upsurge and soil compaction, may change the aspect of wide zones; sand volcanoes even more than 6 m in diameter; vertical subsidence even >1 m; large and long fissures due to lateral spreading are common. Metre-high waves develop in still and running waters. Tsunamis may reach the shores with runups exceeding 5 m flooding flat areas for thousands of metres in land. Boulders (diameter in excess of 2–3 m) can be thrown in the air.

This table includes only the definitions of intensities VII–X that are used in the paper.

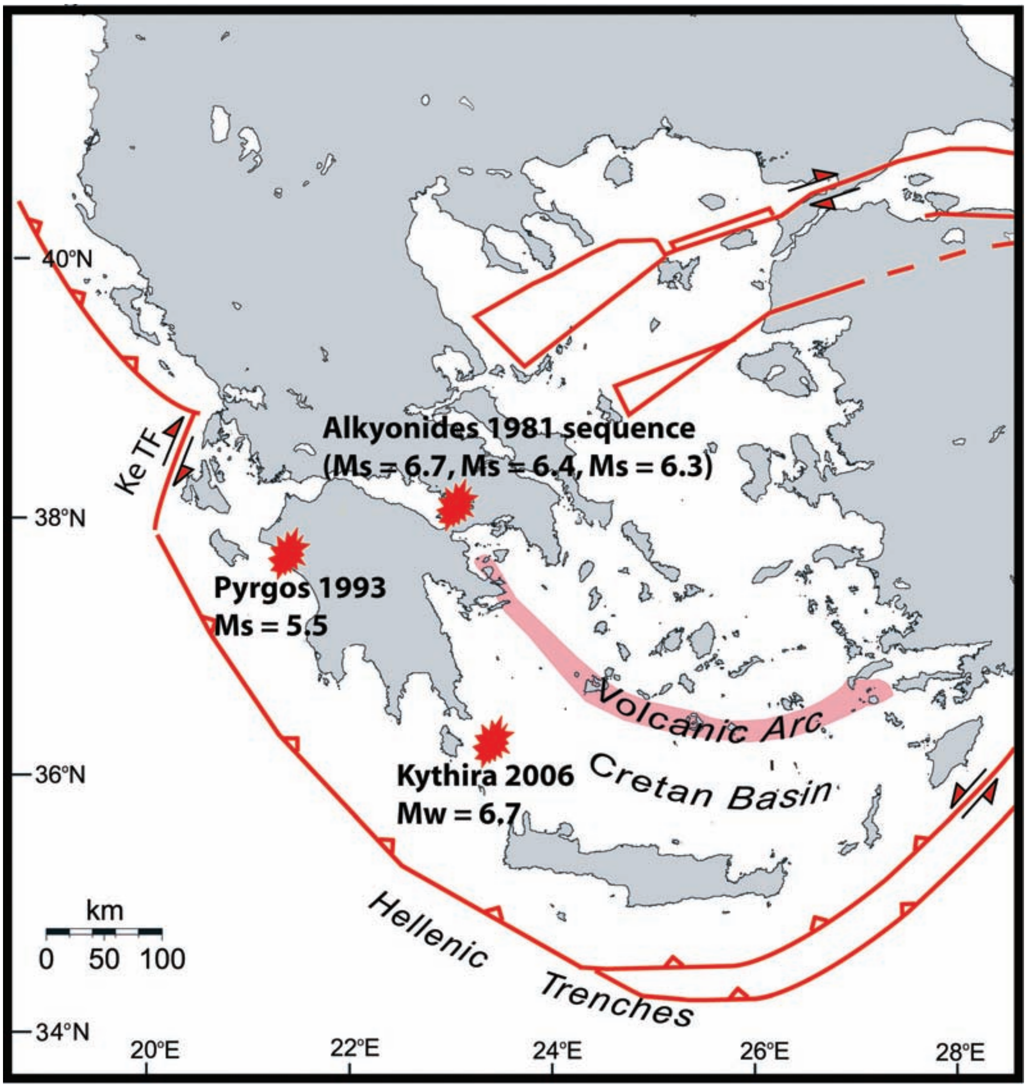

Colour online/colour hardcopy

Fig. 1. Regional map showing the locations of the studied earthquakes within the Hellenic Arc. The 1981 Alkyonides earthquake sequence and the 1995 Pyrgos earthquake were shallow events, whereas the 2006 Kythira event occurred on the subduction zone with a focal depth of about 70 km.

Papanikolaou *et al.* 2007), therefore the generation of a Ms = 5.5 thrust event remains a question. Nevertheless, its focal depth (15 km as proposed by Stavrakakis (1996), but not accurately known) implies that it could also be related to the subduction processes of the Hellenic Trench that is situated approximately 70 km to the west. The subduction zone as imaged by Laigle *et al.* (2002) dips at a very low angle up to the Greek mainland where at about 15 km depth the dip of the interplate reflector becomes steeper, forming a deep ramp. The predominant stress field in the offshore area around Zakynthos and Western Peloponnese has been regarded as compressional (e.g. Papazachos 1990) although more recent studies show a predominant dextral strike slip faulting making the situation even more complicated (e.g. Kiratzi & Louvari 2003; Roumelioti *et al.* 2004). Therefore, it is possible that near the coast there is an extensional regime over the upper 10–12 km, whereas at deeper depths there is either a prevailing compressional regime due to the subducting plate (e.g. Laigle *et al.* 2002) or a dextral shear zone that may be linked to the major neighbouring Kefalonia strike-slip

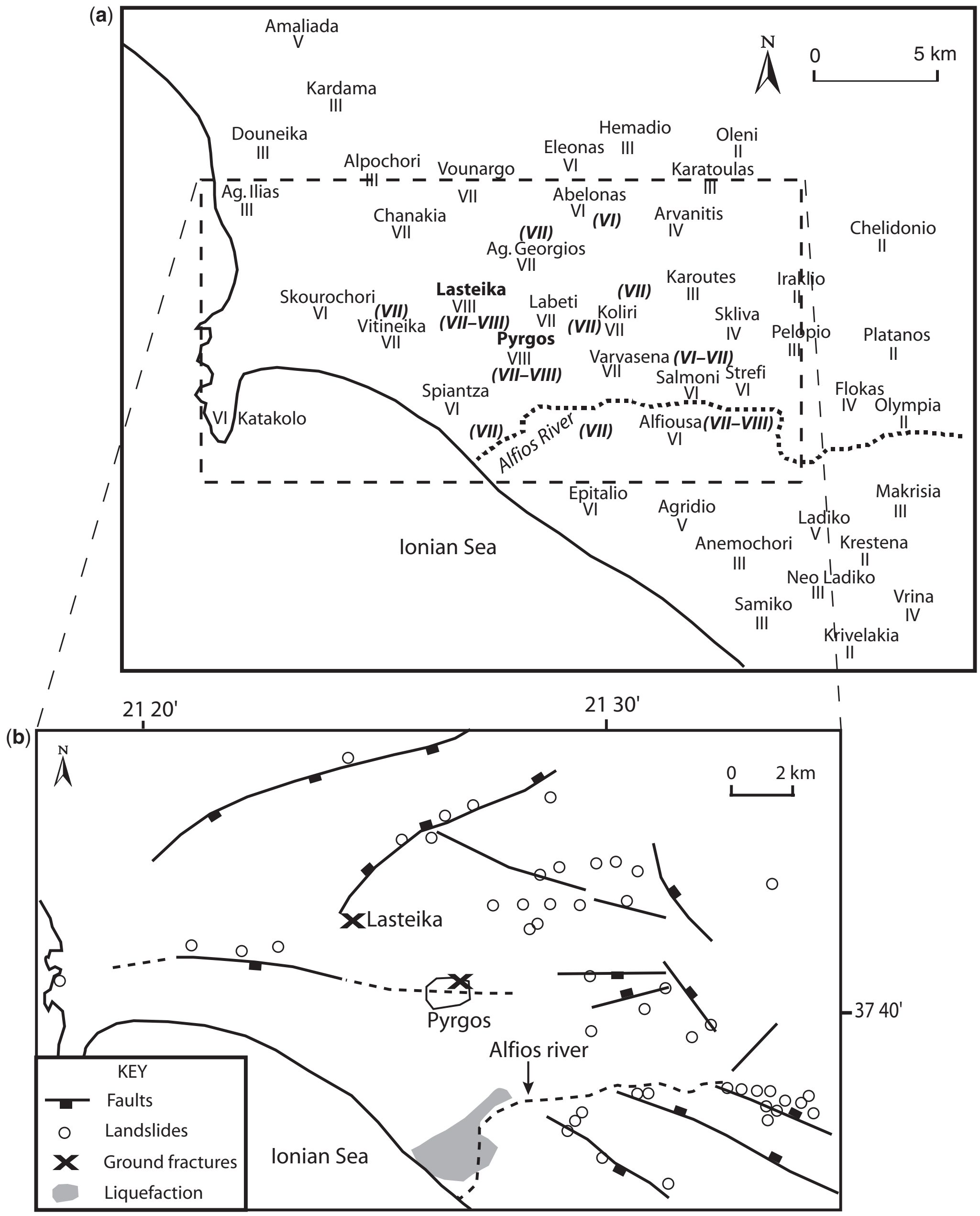

Fig. 2. (**a**) The EMS 1992 (Lekkas *et al.* 2000) and the ESI 2007 scale (this study) distribution of the 1993 Pyrgos earthquake. The ESI 2007 values are in bold italics in parentheses. (**b**) Map of the environmental effects. Ground fractures and liquefaction from Lekkas (1994) and Lekkas *et al.* (2000); landslide localities from Koukouvelas *et al.* (1996).

fault (e.g. Kiratzi & Louvari 2003). The 1993 Pyrgos foreshock activity took place on the SW coast, the main shock under the town of Pyrgos, whereas most aftershocks migrated NE and occurred on planes with a predominant NE–SW direction (Stavrakakis 1996). This probably explains the large spatial distribution of reported secondary effects and particularly landslides.

Although the town of Pyrgos extends over a relatively limited area of about 4 km^2, the distribution

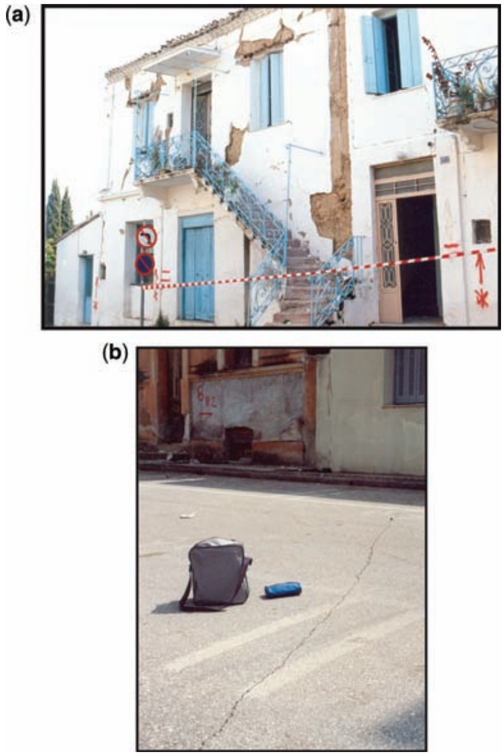

Colour online/ colour hardcopy

Fig. 3. (**a**) View of the damage inflicted in a traditional two-storey, stone masonry building. Several similar buildings suffered significant damage in the Pyrgos event. (**b**) Ground ruptures on paved road in the city of Pyrgos.

Q3 of damage was not uniform (Boukovalas *et al.* 1996). Approximately 25% of the buildings experienced severe damage, yet no foundation failures
Q3 were identified (Karantoni & Boukovalas 1997). The Pyrgos event produced practically no damage to modern reinforced concrete buildings (only 22 buildings experienced light damage), but induced significant damage (Fig. 3a) to traditional buildings of adobe, stone or brick masonry (Karantoni &
Q3 Boukovalas 1997). The intensity of seismic motion was affected not only by the local soil conditions, but also by the construction material, the age
Q3 and the storey number of buildings (Boukovalas *et al.* 1996).

Several environmental effects were reported (Fig. 2b). No primary surface ruptures were recorded, but ground fractures were observed at the northeastern part of Pyrgos town (Fig. 3b) and Lasteika village (situated 2 km NW of Pyrgos), cutting both paved roads and cultivated land (Lekkas *et al.* 2000). Fractures were arranged partly en echelon. Towards the NE part of the town fractures were trending ENE–WSW, were about 30 m long and 2–3 cm wide, whereas at Lasteika village fractures were trending east–west and NNW–SSE and were up to 60 m long (Lekkas *et al.* 2000). The 1993 event triggered several landslides, the vast majority of which occurred along fault scarps and steep slopes and mostly in the Alfios southern river bank (Koukouvelas *et al.* 1996). Koukouvelas *et al.* (1996) measured landslides at 47 locations within an area of 145 km^2. Significant liquefaction and subsidence phenomena were observed 5 km SW of the town of Pyrgos in the coastal zone in recent coastal and fluvial deposits covering an area of about 5 km^2 (Lekkas 1996). Soil fractures up to 30 m long and sand boils up to 50 cm in diameter were observed (Lekkas 1994). Finally, subsidence was also observed in alluvial unconsolidated deposits within Pyrgos.

All these environmental effects are depicted in Figure 2b and have been assessed in relation to the ESI 2007 scale (in Fig. 2a, values in bold italics in parentheses). According to these effects the maximum ESI 2007 values (VII–VIII) are observed in the town of Pyrgos and Lasteika village, where ground fractures a few of tens of metres long have been recorded. Even though landslides are scattered along a large area ($>$100 km^2), possibly indicating a maximum intensity of VIII, most of them were small, occurred along unstable slopes and fault scarps, and clustered accordingly in certain localities. Therefore, we assign intensity values in these sites, ranging from VI to VII–VIII, depending on the density of the landslides. Liquefaction phenomena were also reported near the coast and the Alfios delta (soil fractures a

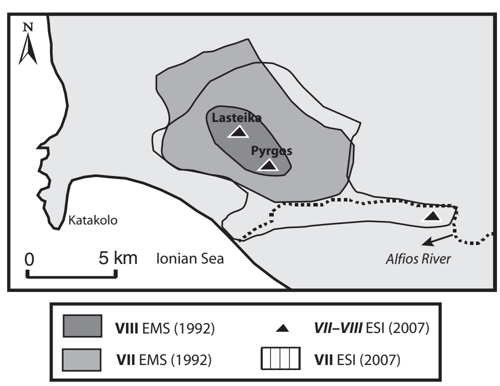

Fig. 4. Comparison of the isoseismal pattern between the EMS 1992 and the ESI 2007 intensity scales. The black triangle symbols show localities where an ESI 2007 intensity VII–VIII degree has been assessed.

few tens of metres long and sand boils up to 50 cm in diameter), a locality highly favourable for liquefaction. These characteristics imply a VII ESI 2007 value.

Maximum EMS 1992 intensity VIII was recorded in the town of Pyrgos and Lasteika village and correlated to the areas where ground ruptures were observed and an ESI 2007 VII–VIII has been assigned (Fig. 2a and Fig. 4). Figure 4 shows the isoseismal pattern of the epicentral region based on the ESI 2007 and the EMS 1992 scales, respectively. The main difference is traced along the Alfios river where liquefaction and sliding phenomena occurred towards the west and the east respectively, extending the ESI 1997 VII isoseismal to the south. However, this difference is mainly due to the lack of EMS 1992 data, since no villages are found in these localities to record an EMS 1992 value. Overall, for the 1993 Pyrgos event, the EMS 1992 and the ESI 2007 scales seem to comply well not only regarding the maximum recorded epicentral intensity, but also with the entire isoseismal pattern.

The 1981 Alkyonides earthquake sequence in the Corinth Gulf

On 24, 25 February and 4 March 1981 three (Ms = 6.7, Ms = 6.4, Ms = 6.3) successive destructive events (20 fatalities and 500 injured) occurred at the eastern end of the Corinth Gulf (Figs 1 and 5) (Jackson *et al.* 1982; Papazachos *et al.* 1982; Taymaz *et al.* 1991). Hubert *et al.* (1996) showed that the last two events of the sequence lie in areas where a positive Coulomb stress increase has been calculated, implying that this earthquake sequence was the result of stress transfer that triggered the second and third events. All three events correspond to normal faulting, accommodating north–south extension. The focal mechanisms that described the coseismic slip at depth (*c.* 10 km), exhibit similar fault plane orientations and kinematics to those measured on the faults at the surface (Morewood & Roberts 2001).

Damages occurred in three different provinces (Beotia, Attica and Corinth) where in total 7701 buildings collapsed or had damage beyond repair,

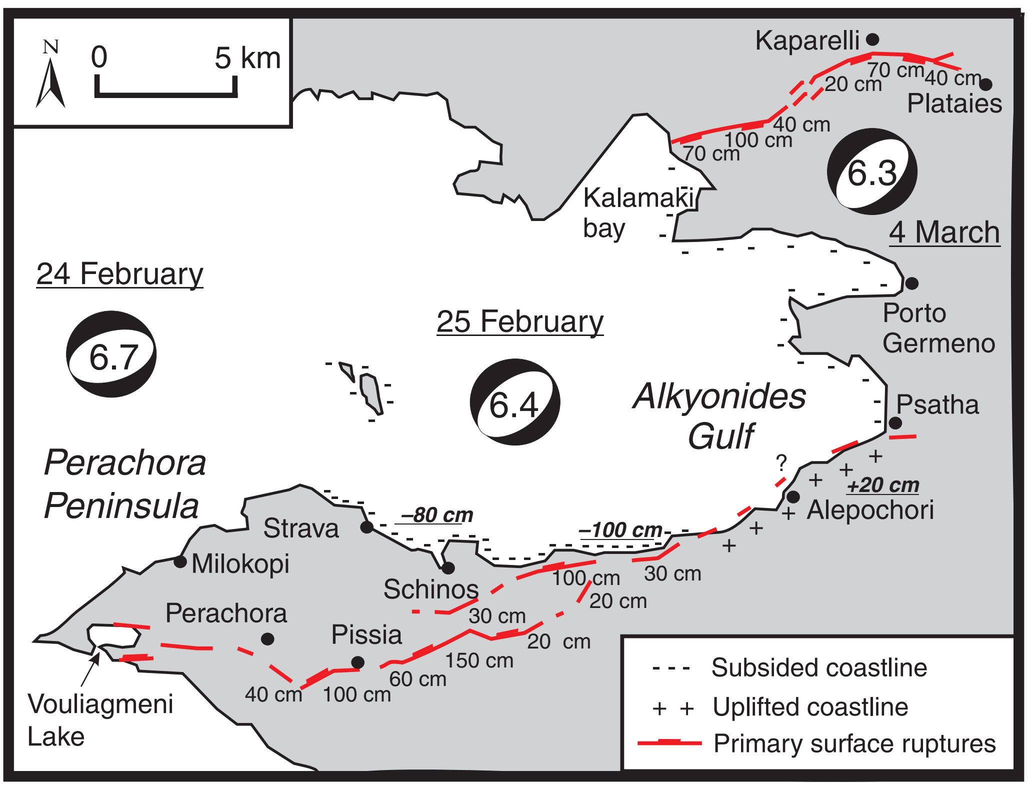

Colour online/colour hardcopy

Fig. 5. The 1981 Alkyonides earthquake sequence, eastern Corinth Gulf. View of the epicentral region with emphasis on the primary surface ruptures and coastal uplift/subsidence. Sketch modified from Jackson *et al.* (1982), Mariolakos *et al.* (1982) and Hubert *et al.* (1996).

Colour online/ colour hardcopy

Fig. 6. (**a**) West of Alepochori up to the western part of the bay of Strava, 50–60 cm of subsidence was observed, flooding up to 50 m of the former shore (Mariolakos *et al.* 1982). (**b**) View of the surface ruptures on the Plataies–Kaparelli fault zone during the 4 March event, producing 50–60 cm of throw (70 cm of displacement).

and 20 954 buildings were severely damaged (Antonaki *et al.* 1988). These events produced numerous earthquake environmental effects (EEE) such as rockfalls, landslides (both onshore and offshore), liquefaction, a weak tsunami wave, significant coastal subsidence and uplift, but most importantly extensive primary surface faulting (Figs 5 and 6b). In particular, in the Pissia Fault, surface ruptures were longer than 10 km and displacements were in the range of 50–70 cm with a maximum recorded value of 150 cm, whereas in the Alepochori Fault displacement was about 100 cm high (Jackson *et al.* 1982; Fig. 5). The 4 March event ruptured the Plataie-Kaparelli Fault Zone (*c.* 10 km of surface ruptures) producing an average 50–60 cm of throw (Jackson *et al.* 1982; Mariolakos *et al.* 1982; Figs 5 and 6b) and a maximum heave and throw of 60 and 120 cm respectively between Kaparelli and Plataies (Papazachos *et al.* 1982). West of Alepochori up to the western part of the Bay of Strava, 60 cm of subsidence was observed, flooding up to 50 m of the former shore (Mariolakos *et al.* 1982; Fig. 6a); however, east of Alepochori coastal uplift was Q4 observed (Jackson *et al.* 1982; Vita-Finzi & King 1985). In Schinos and Strava coastline, there was disagreement on the amount of subsidence recorded, ranging from 50–80 cm (Andronopoulos *et al.* 1982; Mariolakos *et al.* 1982; Hubert *et al.* 1996) Q4 up to 120 and 150 cm (Khoury *et al.* 1983; Vita-Finzi & King 1985). We use a value of 80 cm based on Hubert *et al.*'s (1996) arguments and modelling which show that values higher than 100 cm probably overestimate the coseismic effect.

Subsidence of a few centimetres was also reported away from the epicentral areas in both Loutraki and Kiato coastal area (Andronopoulos *et al.* 1982; see Figs 5 and 7 for localities). Extensive liquefaction occurred at the Kalamaki Bay coastal area (Andronopoulos *et al.* 1982) as well as in Porto-Germeno and in Kineta (Papazachos *et al.* 1982). Ground fissures were reported in Loutraki beach, Vouliagmeni Lake, Porto Germeno, Kiato and Corinth (Papazachos *et al.* 1982).

Submarine slumping in the Alkyonides deep basin and several mass-movement phenomena in the shelf area have also been detected (Perissoratis *et al.* 1984). In particular, a large-scale slump has been documented about 10 km long, 1.5–2 km wide, extending 16 km^2 over a depth of 360 m (Perissoratis *et al.* 1984). Jackson *et al.* (1982) quoted that local people reported a 1 m high tsunami during the main shock in the Alkyonides Gulf. Therefore, it is possible that the tsunami generation can be attributed to the large-scale slumping detected by Perissoratis *et al.* (1984).

All these environmental effects are depicted in Figure 5 and have been assessed according to the ESI 2007 scale (Fig. 8). It should be noted that Q4 subsidence values reported by Vita-Finzi & King (1985) around Milokopi and southwards up to the Q5 town of Loutraki have been debated (Pirazzoli *et al.* 1994; Hubert *et al.* 1996) and have not been considered in this study. Moreover, there is some controversy as to whether the ruptures near Pissia and Schinos should be ascribed to the first or the second event (Jackson *et al.* 1982; King *et al.* 1985; Taymaz *et al.* 1991; Abercrombie *et al.*

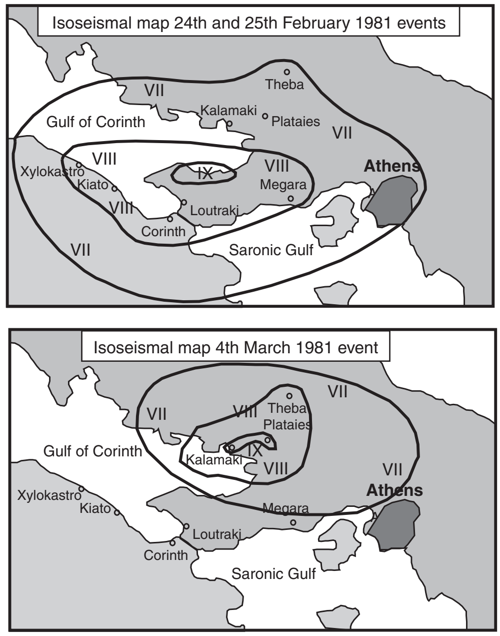

Fig. 7. MS (Mercalli-Sieberg, a version similar to the MCS) intensity distribution of the 1981 Alkyonides earthquake sequence (BGINOA 1981; Antonaki *et al.* 1988). This earthquake sequence had a core of high intensities around the epicentral area and a second maximum of high intensities at 70 km distance, affecting several districts of Athens. On average, Athens experienced intensities VII and VIII; however, in some boroughs and building blocks intensities up to IX were also recorded. Q7

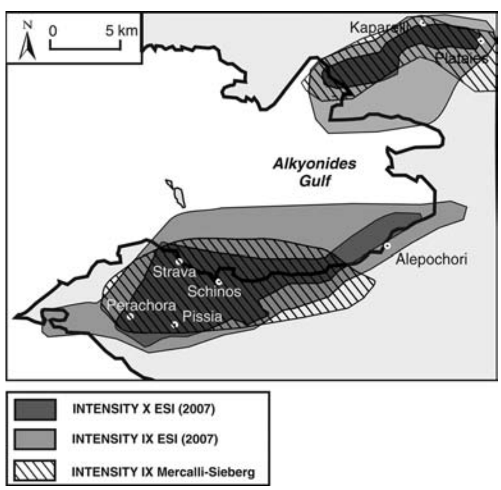

Fig. 8. Comparison of the isoseismal pattern between the MS and the ESI 2007 intensity scales.

1995; Hubert *et al.* 1996), as both occurred at night and only a few hours apart. However, for our study this makes no difference since these two events cannot be separated in terms of their macroseismic effects.

Following the above descriptions a maximum epicentral ESI 2007 value of X is determined in several sites (Fig. 8) and particularly along strike the primary surface ruptures in Pissia, Schinos and in Kaparelli–Plataies where they exceeded a few tens of centimetres in height. Intensity X has also been allocated along the coastal zone from Strava up to Alepochori, where significant subsidence ranging from a few decimetres up to 100 cm has been recorded. Intensity IX is mainly assigned in areas where the surface ruptures were a few tens of centimetres high. Finally, intensity VIII was widely assessed affecting a large area where ground ruptures, extensive landslides, rockfalls and liquefaction phenomena have been observed.

Maximum MS (Mercalli–Sieberg) intensity values (a version similar to the MCS) were also recorded in all villages that were in close proximity to the activated faults (Fig. 8; Perachora IX–X, Plataies IX–X, Schinos IX, Pissia IX, Kaparelli IX). However, no intensity X has been assigned and most of the epicentral villages recorded an epicentral intensity IX (Fig. 8). Figure 8 shows the different isoseismic patterns of the epicentral region based on the ESI 2007 and the Mercalli–Sieberg scales, respectively. Differences are noteworthy, but not substantial. It should be noted that surface geology played a decisive role in the damage distribution and had a significant effect on the intensity observed at a site. On average, under similar circumstances sites located on soil foundations experienced about one intensity degree more shaking than sites located on rock foundations, whereas sites on Neogene sediments experienced about half a degree greater intensity than sites located on rock foundations (Tilford *et al.* 1985).

These shallow normal faulting earthquakes affected not only the Perachora Peninsula (maximum intensity IX–X), Plataies (IX–X) or Kaparelli (IX), but also the city of Athens, located 70 km to the east, where tens of buildings collapsed in certain town districts (Fig. 7). As a result, this earthquake sequence had an anomalous intensity distribution with a core of high intensities around the epicentral area and a second maximum of high intensities at 70 km distance, affecting several districts of Athens. On average, Athens experienced intensities of VII and VIII; however, in some boroughs and building blocks, intensities up to IX were also recorded. In particular, in Athens 1175 buildings collapsed or had to be demolished after the earthquake, whereas 7824 buildings experienced severe damage (Antonaki *et al.* 1988). The degree of damage changed abruptly over short distances due to surface geology. In Athens, the area of damage was highly localized in the boroughs of Chalandri, Anthoupoli, Moschato, Aigaleo, Nea Ionia and Nikaia (suburbs of Athens) mainly due to poor local site conditions (mostly fluvial and alluvial deposits). In particular, in the Chalandri district buildings were of good quality. The highest percentage of damage to single-and two-storey buildings occurred where the depth to bedrock (less than 40 m) and thickness of recent sediments (less than 10 m) were minimum, whereas for the multistorey buildings the higher damage occurred where the depth to bedrock was maximum (greater than 40 m) and the thickness of recent deposits from 5 to 15 m (Christoulas *et al.* 1985). Therefore, damage to multistorey buildings occurred because the dominant period of the soil was approximately equal to the dominant period of these buildings (Christoulas *et al.* 1985).

The 2006 Kythira earthquake

On 8 January 2006 a thrust faulting event $M_w = 6.7$ with considerable strike-slip motion occurred in southwestern Greece (European Mediterranean Seismological Centre, unpubl. data; Konstantinou *et al.* 2006). This event is related to the Hellenic subduction zone (Fig. 1) and the epicentre was located a few tens of kilometres east of the island of Kythira with focal depth estimated at 70 km (United States Geological Survey, unpubl. data). The event was felt throughout Greece and the eastern Mediterranean in general (from Southern Italy and Dalmatian coasts, to Bulgaria, Turkey, Jordan, Israel and Egypt).

No casualties were reported and damage was restricted to the village of Mitata on the island of Kythira (Fig. 9a). Several old stone masonry buildings experienced significant damage (including a few collapses; Fig. 10b); however, modern reinforced concrete buildings did not suffer any damage. The metropolitan church located in the village square sustained severe damage (Fig. 10a) and several stone fences collapsed. A number of rockfalls, landslides and fractures disturbed the local road network (Fig. 11b, c and d), affecting an area of about 15 km^2. However, they were of limited size (Fig. 11d). Fractures a few meters long were observed on paved roads within the village (Fig. 11a). The biggest landslide affected Mitata village square that was partly detached (Fig. 11b), involving a collapsing volume of about 5000 m^3 (Fig. 12; Lekkas & Danamos 2006). Several masses of rock (*c*. 500 m^3 each) were detached for about 100 m and were accumulated at the base of the slope on the Mitata–Viaradika road. A few more rockfalls were observed along the

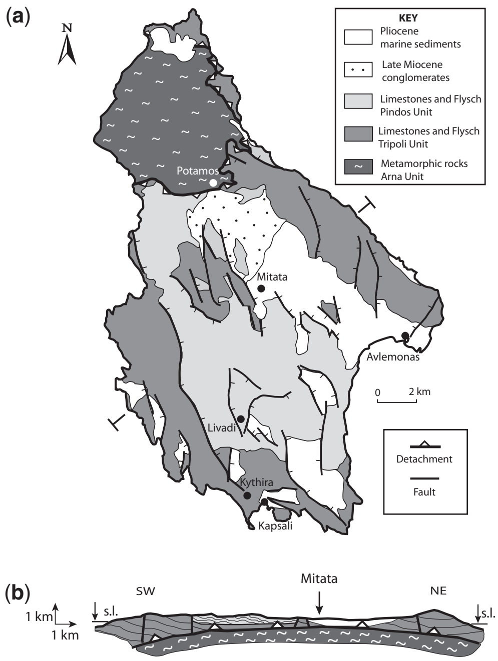

Fig. 9. (**a**) Geological map of Kythira island (modified from Papanikolaou & Danamos 1991). (**b**) Cross-section across Mitata village. Mitata village is situated on the immediate hanging wall of an active fault. In addition, it is founded on Pliocene marine sediments that rest on a large NNW–SSE trending detachment fault that lies a few hundred metres below the village separating the non-metamorphic rocks from the underlying metamorphic rocks of the Arna Unit.

remaining road network of the island, but no liquefaction phenomena were recorded. Therefore, remarkable EEE were observed only in the village of Mitata in compliance with the damage distribution. It is interesting to note that even though several villages of the island are equidistant from the epicentre, only Mitata village was damaged and experienced some noteworthy EEE. In particular, in Potamos village, situated only 35 km from the epicentre (Fig. 9a), the reported MM intensity was V+, whereas in Mitata village situated *c.* 40 km the intensity was VII+ (Konstantinou *et al.* 2006). This intensity distribution was likely due to: (a) the poor foundation conditions of the village, (b) its proximity to an active neotectonic fault that bounds a Late Miocene–Pliocene basin (Papanikolaou & Danamos 1991), and (c) the presence of a large detachment fault at a few hundred metres below the village (Papanikolaou & Danamos 1991). On the other hand, Potamos village is founded on the metamorphic rocks of the Arna Unit and consequently is located under the footwall block of the detachment (Fig. 9).

The NE–SW trending cross-section across Mitata village (Fig. 9b) shows the geological structure of the area. The village of Mitata is founded on Pliocene marine sediments that rest on a large NNW–SSE trending detachment fault. This detachment, situated a few hundred metres below the village, separates the non-metamorphic rocks from the underlying metamorphic rocks of the Arna Unit, belonging to the East Peloponnesus detachment system (Papanikolaou & Royden 2007). Finally, the village of Mitata is situated in the immediate hanging wall of an active NW–SE normal fault. The village of Mitata was devastated (intensity XI) by a similar deep-sourced (*c.* 80 km), but significantly stronger M = 7.9 event that occurred in 1903 (Papazachos & Papazachou 1997). Then, the newly constructed church and the school building collapsed and several ground fissures were reported, of which one was 200 m long and 1 cm wide (Papazachos & Papazachou 1997). This past event also confirms that Mitata village is founded in unfavourable geological conditions.

Based on the environmental effects, an ESI 2007 maximum epicentral intensity of VII–VIII has been assigned, which is similar to the MM reported intensity value.

Discussion: advances and limitations of the ESI 2007 scale

The ESI 2007 scale has been tested in earthquakes that: (i) had different source characteristics (magnitude, focal mechanism and focal depth) and (ii) produced a variety of environmental effects (primary surface faulting, minor and major secondary effects), which help us obtain a spherical view of its performance.

The ESI 2007 scale has been easily applied, leaving no question marks or 'grey' areas in all three examples. Above the intensity VII degree when environmental effects become prominent, the ESI 2007 scale can define the intensity degree with a high level of accuracy as also shown in several recent and historic earthquakes worldwide (e.g. Serva *et al.* 2007; Tatevosian *et al.* 2007). Overall, the 1993 Pyrgos and the 2006 Kythira events demonstrate that for moderate intensity levels (VII and VIII) the ESI 2007 and the traditional scales compare fairly well. On the other hand, the 1981 Alkyonides earthquake sequence demonstrates that there is inconsistency between ESI 2007 and traditional scales for the high intensity values (IX, X). This seems to agree with similar examples worldwide, emphasizing the importance and the increasing accuracy of the ESI 2007

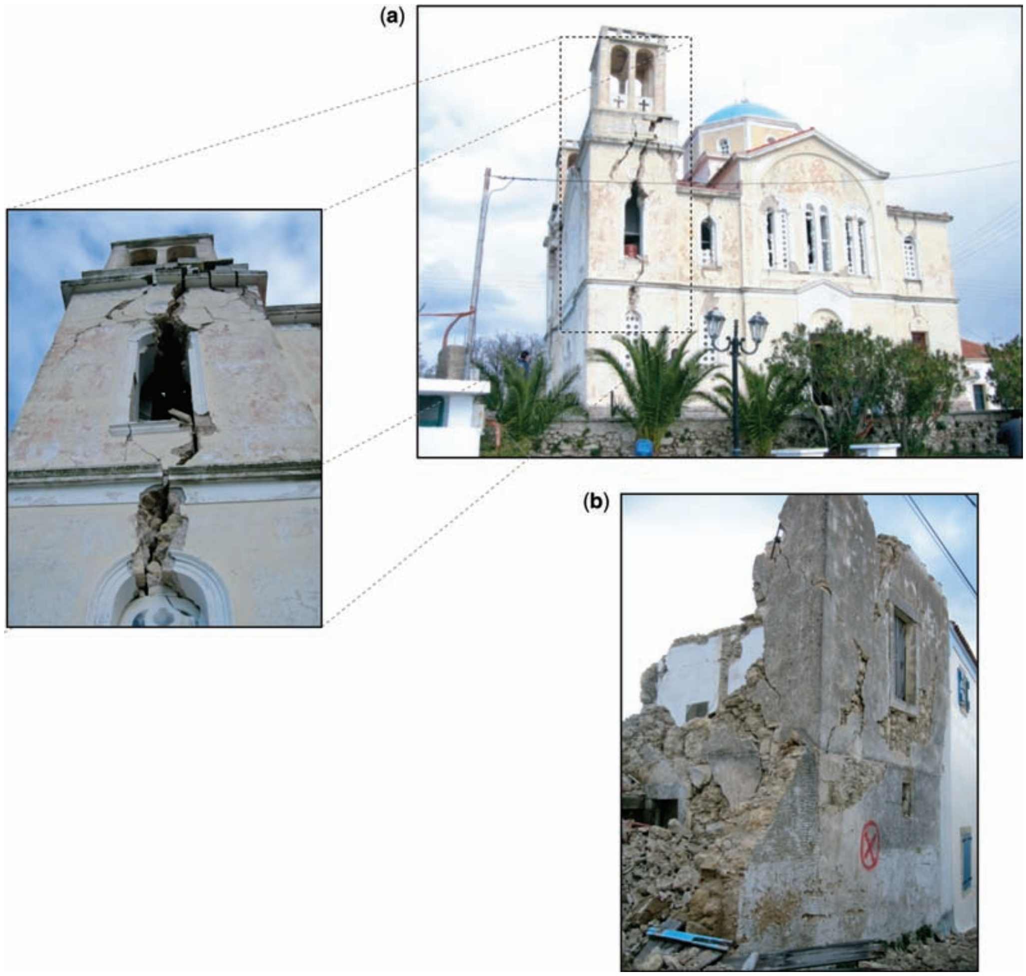

Colour online/colour hardcopy

Fig. 10. (**a**) Photos of the damage inflicted on the metropolitan church of Mitata village. The church, located in the village square, is constructed of porous limestone blocks cemented with lime wash without concrete columns and experienced significant damage. Severe damage was also inflicted at both bell towers. (**b**) A few collapses of old plain stone masonry buildings were recorded at Mitata.

scale towards the highest levels of the scale in the epicentral area (e.g. Michetti *et al.* 2007; Serva *et al.* 2007).

In particular, for the 1993 Pyrgos event, the EMS 1992 and the ESI 2007 scales seem to comply well regarding not only the maximum recorded epicentral intensity, but also with the overall isoseismal pattern. Nevertheless, it should be mentioned that no villages were founded near the landslide or the liquefaction-prone areas, otherwise it is possible that the traditional intensities would have recorded a higher epicentral intensity value.

In addition, even for the 2006 Kythira deep-sourced event, the ESI 2007 and the traditional macroseismic scales correlate well, suggesting a maximum VII–VIII intensity. A question arises as to whether a more destructive deep-sourced event such as the M = 7.9 earthquake that occurred in Kythira in 1903 ($I_0 = XI$; Papazachos & Papazachou 1997) would have been correctly interpreted in the ESI 2007 scale, since no primary surface ruptures would have been observed to imply a higher intensity value and reported ground fissures were of limited length. In such deep not 'linear morphogenic events' (e.g. Caputo 2005), where ruptures cannot reach the surface, the ESI 2007 intensity level should be correlated with the area where severe environmental effects have been recorded. However, in such cases uncertainties are expected to be higher, implying that the assessment

Fig. 11. (**a**) Ground ruptures on paved road at the village of Mitata. (**b**) View of the landslide that affected Mitata village square, which was partly detached, involving a collapsed volume of about 5000 m^3. (**c**) View of rockfalls disturbing the road. (**d**) View of a minor landslide blocking the road.

Colour online/ colour hardcopy

of the ESI 2007 scale should probably be considered less precise for deep events.

In the 1981 Alkyonides example, the ESI 2007 intensity scale provides not only a slightly higher maximum epicentral intensity (X), but also a different spatial distribution of the isoseismals, compared to the traditional scales. This implies that current traditional scales possibly underestimate the ‘strength’ of this kind of earthquake sequence. This occurs partly because the epicentral area, where significant EEE were recorded, was relatively sparsely populated. Indeed, only the small villages of Schinos, Pissia Kaparelli and Plataies were situated a few hundred metres up to a few kilometres

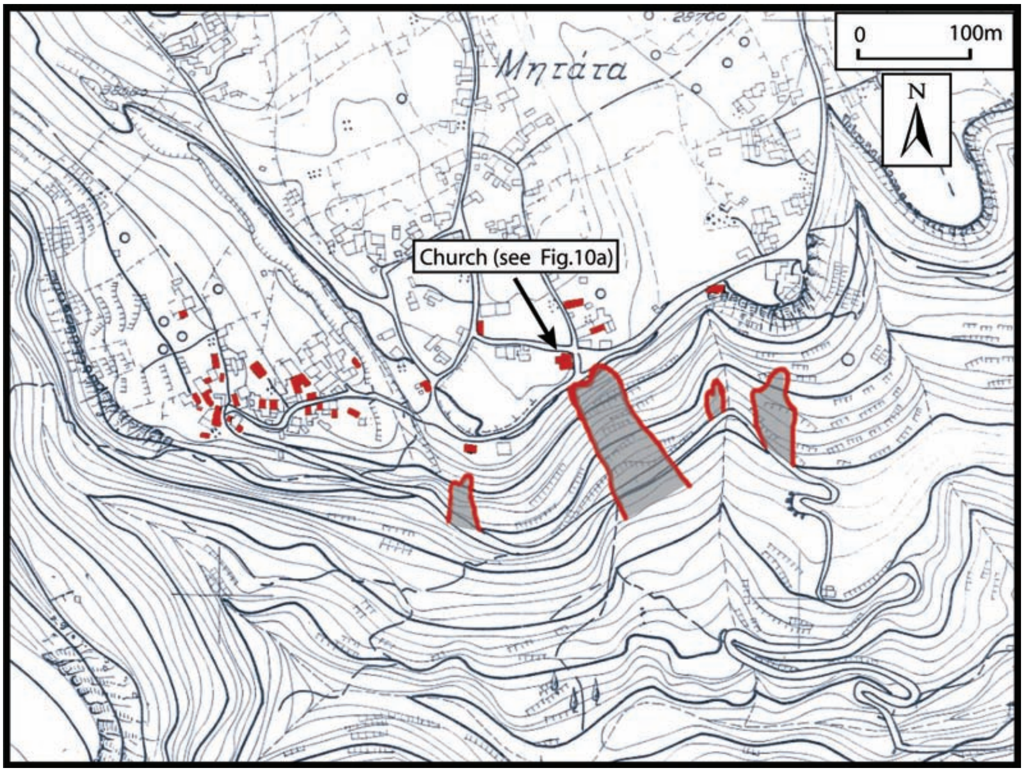

Colour online/ colour hardcopy

Fig. 12. Landslide (grey areas) and damage (bold blocks) distribution around Mitata village mapped at a 1:5000 scale (Lekkas & Danamos 2006). Thick contours represent intervals of 20 m and thin contours intervals of 4 m.

away from the localities where significant offsets (>20 cm) have been observed. Although Kaparelli was the most proximal village to the surface ruptures of the third event and is founded on a rather unfavourable geological site (Pleistocene fluvial, breccia and slope deposits), it experienced intensity IX. This occurred because it is situated in the immediate footwall of the fault and thus experienced less shaking. Moreover, in Schinos village several houses were founded on the ophiolitic bedrock and experienced minor to moderate damages (Andronopoulos *et al.* 1982), thus lowering the epicentral maximum intensity. The same is probably true for Pissia since part of the village is founded on Holocene scree and Pleistocene breccia deposits, but the remaining part is on the Alpine basement. In addition, Plataies village is also founded on Mesozoic limestones. Tilford *et al.* (1985), following a survey in the area, suggested that surface geology significantly influenced the damage distribution and calculated that on average, buildings located on soil foundations experienced about one degree of intensity more than those located on rock foundations. Previous remarks may explain why an epicentral intensity of X has not been fully implemented. From this perspective, it is argued that for the Alkyonides example the ESI 2007 scale is probably more appropriate for drawing isoseismals of intensity IX and X in the epicentral area.

As far as the far field effects are concerned, there is an inconsistency for the town of Athens between the EEE, which were negligible, and the significant damage that occurred in some town districts. This inconsistency for the far field of the 1981 earthquake sequence between the ESI 2007 and the Mercalli intensity scale can be attributed to several reasons. It could be that intensive earthquake environmental related effects have not been expressed or even recorded in Athens, due to the strictly localized area of damage and its limited geographical coverage. However, it is argued that this inconsistency is probably due to the structural response of multistorey buildings, the bedrock geology and the local site effects (e.g. Tilford *et al.* 1985) in accordance with the long distance from the epicentre. In this case there was a long period resonance because the dominant period of the soil was approximately equal to the dominant period of certain buildings, causing severe damage (e.g. Christoulas *et al.* 1985). In addition, considering that Athens experienced three strong successive events over a few days, the weakness and the vulnerability of the buildings would have been substantially increased. This comparison for the far field effects may be inappropriate since no EEE were recorded in the far field, even though structural damage did occur. However, it is also important to establish that the ESI 2007 scale should be used predominantly in the epicentral area and thus may not accurately describe damage in the far field. Nevertheless, the Kythira example shows that the far field effects are in compliance with the EEE.

A few other events have been studied in Greece and reassessed in terms of the ESI 2007 scale. Papathanasiou & Pavlides (2007) found that in the 2003 Lefkada earthquake (Ms = 6.4), the traditional intensities tend to underestimate the ground shaking because the strengthening of buildings, due to the strict seismic code in the area, resulted in better performance under ground shaking. However, two similar events that occurred in the past before the provision of the seismic code had similar intensity values as the ESI 2007 scale. The 1988 Elia earthquake (Ms = 5.9) in NW Peloponnese shows that the traditional intensities were similar to the ESI 2007 scale, whereas in the 1999 Athens event (Ms = 5.9), the ESI 2007 intensities underestimated the impact of the earthquake (Focaefs & Papadopoulos 2007). The 2003 Lefkada (Papathanasiou & Pavlides 2007), the 1999 Athens (Focaefs & Papadopoulos 2007) and the 1981 earthquake sequence (this study) indicate that when the ESI 2007 and the traditional intensity scales disagree, the intensity has to coincide with the highest value between these two independent estimates (see also Serva *et al.* 2007; Michetti *et al.* 2007).

Another important issue that has arisen from the 1981 Alkyonides earthquake sequence is the different isoseismal distributions recorded by several research groups. In several epicentral villages, reported intensity values differ from half (e.g. Perachora and Pissia) up to one degree (Schinos). For example, in Schinos village intensity recordings varied from VIII–IX (Papazachos *et al.* 1982), IX (BGINOA 1981) up to IX–X (Andronopoulos *et al.* 1982), providing a rather confusing pattern. This difference can be attributed to several causes. It may be: (i) due to the subjective interpretation of damages or (ii) due to the subjectivity in allocating the predominant damage in a site, or (iii) because the assigned intensities correspond to the maximum observed intensity rather than the mean. From this perspective, the ESI 2007 scale is probably easier to implement and more precise in quantifying macroseismic effects, offering a higher objectivity in the process of assigning intensity values.

Finally, the use of many different intensity scales worldwide (e.g. MM, MCS, MSK, JMA), which are also constantly updated (e.g. EMS 1992) indirectly demonstrates the inefficiency of current earthquake intensity scales in describing the macroseismic earthquake effects.

The ESI 2007 scale and implications for seismic hazard assessment

Intensity is an important seismic hazard parameter. The isoseismal maps are used to derive empirical relations for the decrease of intensity with distance, which then are incorporated into the attenuation laws and used to assess the seismic hazard. One fundamental question that will be posed is why introduce another intensity scale without clear outcomes to the seismic hazard assessment? In this section we show how the ESI 2007 scale could prove beneficial for seismic hazard assessment by reducing the uncertainty in the empirically based attenuation laws and demonstrate: (i) how large the uncertainty is and (ii) how significant is this uncertainty for the seismic hazard maps.

Intensity attenuates with increasing distance from the earthquake source, at first rapidly and then more slowly. Therefore, in order to define the seismic hazard at a given site, it is necessary to know the expected attenuation of intensity with epicentral distance. Thus, attenuation curves are simple empirical relationships that give the largest amplitudes as a function of epicentral intensity and/or earthquake magnitude with distance and are compiled based on the statistical elaboration of historical and instrumental data. However, there is a large variation in the data, which adds uncertainty in the seismic hazard assessment. This variation is nicely portrayed in an empirical magnitude–intensity database compiled by D'Amico *et al.* (1999), which is presented in Table 2. This database is extracted from instrumental catalogues ranging from 1880 to 1980, covering the whole Mediterranean region. For example, Table 2 shows that epicentral intensity X has been produced by significantly different magnitude events, ranging from M = 6.0 to M = 7.0. It is possible that a portion of this variation in the data stems from the way macroseismic effects have been assessed. Therefore, wherever feasible, by reconstructing the macroseismic field of historical earthquakes, through the use of the ESI 2007 scale, the uncertainties may be significantly reduced.

Evidently, apart from the attenuation/amplification relationships, uncertainty in seismic hazard assessment stems from several other factors such as the fault geometry, slip rates, the earthquake occurrence model used etc. However, it seems that

Table 2. *Distribution of the magnitude values for each intensity class in the Mediterranean region*

Intensity	Number of events	Lower magnitude	Upper magnitude	Mean magnitude (Ms)	
VIII	161	5.0	5.9	5.4	
VIII–IX	20	5.7	6.3	6.0	
IX	53	5.8	6.7	6.2	
IX–X	**5**	**6.3**	**6.9**	**6.5**	Q15
X	**18**	**6.0**	**7.0**	**6.6**	

Modified from D'Amico *et al.* 1999

seismic hazard maps are also highly sensitive to the attenuation relationship used. In particular, in some cases uncertainty is large enough so that it overshadows the other factors. For example, following Table 2 on average a M = 6.5 earthquake is expected to produce an epicentral intensity IX or X (or IX–X). However, the exact value of the epicentral intensity (whether IX or X) is crucial for the determination and modelling of the area affected around the epicentre and the attenuation relationships. Indeed, historical data of macroseismic intensity versus epicentral distance published by Grandori *et al.* (1991), covering the whole of the Apennines in Italy, show that earthquakes with epicentral intensity IX ($I_0 = 9$) have a mean radius of 6–7 km for the intensity IX isoseismal, whereas earthquakes with epicentral intensity X ($I_0 = 10$) have a mean radius of 20–21 km for the isoseismal IX (Fig. 13a). Similar values have been reported for other regions such as the Sino-Korean craton (Lee & Kim 2002; Fig. 13b). The significance of this uncertainty can be portrayed and easily assessed in quantitative fault-specific seismic hazard maps from geological fault slip-rate data (Papanikolaou 2003; Roberts *et al.* 2004). Roberts *et al.* (2004) used in Lazio-Abruzzo, central Italy, an average value of 12.5 km radius for the modelled isoseimal IX in the central Appenines, whereas Papanikolaou (2003) used the average value of 12.5 km and an extreme upper value of 20 km, running a sensitivity analysis for the southern Apennines. Sensitivity analysis showed that the error introduced by the implied uncertainty in the dimensions of modelled isoseismals is significantly larger than the fault throw-rate error (of ±20%). This is remarkable because it shows that input parameters such as the isoseismal dimensions, which themselves are derived from attenuation relationships, influence the results more significantly than the uncertainty implied from the fault throw-rate data which govern the earthquake recurrence. Therefore, further evaluation that could constrain the isoseismal dimensions and the attenuation relationships will prove beneficial in limiting the uncertainties implied in the seismic hazard analysis for the regions of central and southern Apennines.

It should be noted that the complication and uncertainty in earthquake ground motion and consequently in the attenuation/amplification relationships is not only related to the way intensity values have been assigned and isoseismal lines

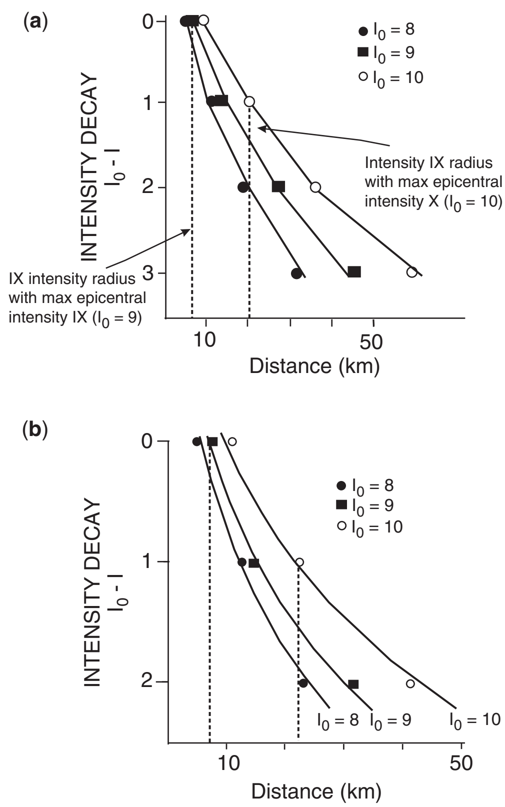

Fig. 13. Attenuation laws for: (**a**) the Apennines in Italy (modified from Grandori *et al.* 1991) and (**b**) the Sino-Korean peninsula (modified from Lee & Kim 2002). Attenuation laws are derived from the statistical elaboration of historical and instrumental data. The Apennines example shows that earthquakes with epicentral intensity IX ($I_0 = 9$) have a mean radius of 6–7 km for the intensity IX isoseismal, whereas earthquakes with epicentral intensity X ($I_0 = 10$) have a mean radius of 20–21 km for the isoseismal IX.

have been drawn, but emerges from several factors, which are critical but not accurately known. These factors vary from source to source, path to path and from site to site introducing a large scatter in numerical values of ground motion (e.g. Hu *et al.* 1996). Moreover, some of these factors are 'highly interdependent' making it difficult to separate near-surface effects from deeper basin effects (Field *et al.* 2000). Studies on the prediction of ground motion and the site effects suggest that site response has a large intrinsic variability with respect to source location (Hartzell *et al.* 1997). The intrinsic variability is caused by basin-edge induced surface waves, focusing and defocusing effects and scattering in general that cannot be reduced in any model (Field *et al.* 2000). Therefore, there is little hope that all uncertainties implied by the attenuation/amplification relationship can be fully reduced. However, it is also probable that part of this uncertainty stems from the intensity evaluation. The ESI 2007 scale offers higher objectivity in the process of assessing macroseismic intensities than traditional intensity scales that are influenced by human parameters. Thus, the ESI 2007 scale can compare not only events from different settings, but also contemporary and future earthquakes with historical and even pre-historical events. This occurs because the ESI 2007 scale follows the same criteria/environmental effects for all events that are independent of the local economy and cultural setting through time. Therefore, a reappraisal of historical earthquakes so as to constrain the INQUA intensity scale may prove beneficial for the seismic hazard assessment by reducing the uncertainty implied in the attenuation laws.

Conclusions

The ESI 2007 scale incorporates the advances and achievements of palaeoseismology and earthquake geology, forming an objective and easily applied tool for measuring the earthquake strength, particularly in the epicentral area.

The ESI 2007 intensity values and the spatial distribution of the isoseismals for the 1993 Pyrgos and the 2006 Kythira events are similar to those resulting from the traditional scales, demonstrating that for moderate intensity levels (VII and VIII) the ESI 2007 and the traditional scales compare fairly well. On the other hand, the 1981 Alkyonides earthquake sequence shows that there is an inconsistency between the ESI 2007 and the traditional scales both in the epicentral area, where higher ESI 2007 values have been assigned, and for the far field effects. In the 1981 Alkyonides sequence, the ESI 2007 scale provides not only a slightly higher maximum epicentral intensity, but also a different isoseismal pattern compared to the traditional scales, implying that current traditional scales underestimate the 'strength' of this earthquake sequence. This occurs partly because the epicentral area, where significant EEE were recorded, was sparsely populated. In addition, several villages located in the epicentral region were founded on bedrock sites and others on the footwall block, experiencing less shaking. The 1981 earthquake sequence emphasizes the importance and the increasing accuracy of the ESI 2007 scale towards the highest levels of the scale in the epicentral area. In contrast, the ESI 2007 scale may not accurately describe the damage in the far field. In Athens, situated about 70 km from the epicentre, the EEE were negligible, but several town districts suffered significant damage, because the dominant period of the soil was approximately equal to the dominant period of certain buildings. This example demonstrates once again that when the ESI 2007 and the traditional intensity scales disagree, the intensity has to coincide with the highest value between these two independent estimates.

Earthquake environmental effects provide higher objectivity in the process of assigning intensity values, so that the ESI 2007 scale is the best tool to compare recent, historic and pre-historic earthquakes as well as earthquakes from different tectonic settings. A reappraisal of historical earthquakes, so as to constrain the ESI 2007 scale, may prove beneficial for the seismic hazard assessment by reducing the uncertainty implied in the attenuation laws.

We thank Alessandro Michetti for discussions concerning the application of the ESI 2007 scale. Reviews from Spyros Pavlides and Riccardo Caputo improved the paper.

References

Abercrombie, R., Main, I. G., Douglas, A. & Burton, P. W. 1995. The nucleation and rupture process of the 1981 Gulf of Corinth earthquakes from deconvolved broad band data. *Geophysical Journal International*, **120**, 393–405.

Andronopoulos, B., Eleftheriou, A., Koukis, G., Rozos, D. & Angelidis, C. 1982. Macroseismic, geological and tectonic observations in the area affected by the earthquakes of the Corinthian Gulf (February–March 1981). *International Symposium on the Hellenic Arc and Trench (H.E.A.T.)*, **1**, 19–34.

Antonaki, R., Vlachos, I. *et al.* 1988. *Earthquake Economic Impact – Insurance*. Report of Earthquake Planning and Protection Organization [in Greek]. **Q8**

Bouckovalas, G., Anagnostopoulos, A., Kapenis, A. & Karantoni, T. 1996. Analysis of soil effects and distribution of damage from the Pyrgos 1993 (Greece) earthquake. *Geotechnical and Geological Engineering*, **14**, 111–128.

Caputo, R. 2005. Ground effects of large morphogenic earthquakes. *Journal of Geodynamics*, **40**, 113–118.

Christoulas, S. G., Tsiambaos, G. K. & Sabatakakis, N. S. 1985. Engineering geological conditions and the effects of the 1981 earthquake in Athens, Greece. *Engineering Geology*, **22**, 141–155.

Coburn, A. & Spence, R. 2002. *Earthquake Protection*. John Wiley, Chichester.

D'Amico, V., Albarello, D. & Mantovani, E. 1999. A distribution-free analysis of magnitude-intensity Q9 relationships: an application to the Mediterranean region. *Physics and Chemistry of Earth*, **24**, 517–521.

Dziewonski, A. M., Ekstrom, G. & Salganik, M. P. 1994. Centroid-moment tensor solutions for January–March 1993. *Physics of the Earth and Planetary* Q10 *Interiors*, **82**, 9–17.

Field, E. H. & SCEC Phase III Working group 2000. Accounting for site effects in probabilistic seismic hazard analyses of southern California: Overview of the SCEC Phase III report. *Bulletin of the Seismological Society of America*, **90**, S1–S31.

Fokaefs, A. & Papadopoulos, G. 2007. Testing the new INQUA intensity scale in Greek earthquakes. *Quaternary International*, **173–174**, 15–22.

Grandori, G., Drei, A., Perotti, F. & Tagliani, A. 1991. Macroseismic intensity versus epicentral distance: the case of Central Italy. *Tectonophysics*, **193**, 165–171.

Grunthal, G. (ed.) 1993. *European Macroseismic Scale 1992 (updated MSK-scale)*. Conseil de l' Europe, Luxemburg, Cahiers du centre Europeen de Geodynamique et de Sismologie **7**.

Hartzell, S., Harmsen, S., Frankel, A., Carver, D. & Meremonte, M. 1997. Variability of site response in the Los Angeles urban area. *Bulletin of the Seismological Society of America*, **86**, S186–S192.

Hu, Y.-X., Liu, S.-C. & Dong, W. 1996. *Earthquake Engineering*. E & FN Spon, London.

Hubert, A., King, G., Armijo, R., Meyer, B. & Papanastasiou, D. 1996. Fault-reactivation, stress interaction and rupture propagation of the 1981 Corinth earthquake sequence. *Earth and Planetary Science Letters*, **142**, 573–585.

Jackson, J. A., Gagnepain, J., Houseman, G., King, G. C. P., Papanimitriou, P., Soufleris, C. & Virieux, J. 1982. Seismicity, normal faulting and the geomorphological development of the Gulf of Corinth (Greece): the Corinth earthquakes of February and March 1981. *Earth and Planetary Science Letters*, **57**, 377–397.

Karantoni, F. V. & Bouckovalas, G. 1997. Description and analysis of building damage due to Pyrgos, Greece earthquake. *Soil Dynamics and Earthquake Engineering*, **16**, 141–150.

Khoury, S. G., Tilford, N. R., Chandra, U. & Amick, D. 1983. The effect of multiple events on isoseismal maps of the 1981 earthquake at the Gulf of Corinth. *Bulletin of the Seismological Society of America*, **73**, 655–660.

King, G. C. P., Ouyang, Z. X. *et al*. 1985. The evolution of the Gulf of Corinth (Greece): an aftershock study of the 1981 earthquakes. *Geophysical Journal of the Royal Astronomical Society*, **80**, 677–683.

Kiratzi, A. & Louvari, E. 2003. Focal mechanisms of shallow earthquakes in the Aegean Sea and the surrounding lands determined by waveform modeling: a new database. *Journal of Geodynamics*, **36**, 251–274.

Konstantinou, K. I., Kalogeras, I. S., Melis, N. S., Kourouzidis, M. C. & Stavrakakis, G. N. 2006. The 8 January 2006 Earthquake (Mw 6.7) offshore Kythira island, Southern Greece: Seismological, strong motion and macroseismic observations of an intermediate-depth event. *Seismological Research Letters*, **77**, 544–553.

Koukouvelas, I., Mpresiakas, A., Sokos, E. & Doutsos, T. 1996. The tectonic setting and earthquake ground hazards of the 1993 Pyrgos earthquake, Peloponnese, Greece. *Journal of the Geological Society London*, **153**, 39–49.

Laigle, M., Hirn, A., Sachpazi, M. & Clement, C. 2002. Seismic coupling and structure of the Hellenic subduction zone in the Ionian islands region. *Earth and Planetary Science Letters*, **200**, 243–253.

Lee, K. & Kim, J.-K. 2002. Intensity attenuation in the Sino-Korean Craton. *Bulletin of the Seismological Society of America*, **92**, 783–793.

Lekkas, E. 1994. Liquefaction – Risk zonation and urban development in Western Peloponnese (Greece). *Proceedings of 7th International Congress, International Association of Engineering Geology*, 2095–2102. Q11

Lekkas, E. 1996. Pyrgos earthquake damages (based on E.M.S.-1992) in relation with geological and geotechnical conditions. *Soil Dynamics and Earthquake Engineering*, **15**, 61–68.

Lekkas, E. & Danamos, G. 2006. Preliminary observations of the January 8, 2006 Kythira island (SW Greece) earthquake (Mw = 6.9). *Newsletter E.E.R.I.*, 1–20. Q12

Lekkas, E., Fountoulis, I. & Papanikolaou, D. 2000. Intensity distribution and Neotectonic macrostructure Pyrgos Earthquake data (26 March 1993, Greece). *Natural Hazards*, **21**, 19–33.

McGuire, R. K. 1993. Computations of seismic hazard. *Annali di Geofisica*, **36**, 181–200.

Mariolakos, I., Papanikolaou, D., Symeonidis, N., Lekkas, S., Karotsieris, Z. & Sideris, C. 1982. The deformation of the area around the eastern Korinthian gulf, affected by the earthquakes of February–March 1981. *Proceedings of International Symposium on the Hellenic Arc and Trench (H.E.A.T.)*, **1**, 400–420. Q13

Melis, N., Tselentis, G. & Sokos, E. 1994. The Pyrgos (March 26, 1993; Ms = 5.2) earthquake sequence as it was recorded by the Patras seismic network. *Bulletin of the Geological Society of Greece*, **30**, 175–180.

Michetti, A. M., Esposito, E. *et al*. 2004. The INQUA scale: An innovative approach for assessing earthquake intensities based on seismically-induced ground effects in natural environment. Special paper *Memorie Descrittive della Carta Geologica D'Italia*, **LXVII**.

Michetti, A. M., Esposito, E. *et al*. 2007. Intensità scale ESI 2007. *In*: Guerrieri, L. & Vittori, E. (eds) *Memorie Descrittive della.* Carta Geologica d'Italia, **74**, Servizio Geologico d'Italia, Dipartimento Difesa del Suolo, APAT, Rome.

Morewood, N. C. & Roberts, G. P. 2001. Comparison of surface slip and focal mechanism slip data along normal faults: an example from the eastern Gulf of Corinth, Greece. *Journal of Structural Geology*, **23**, 473–487.

Papanastasiou, D., Stavrakakis, G. N. & Drakopoulos, J. 1994. A study of the March 26, 1993, Pyrgos earthquake sequence and its tectonic Implications. *Proceedings of the XXIV General Assembly of the European Seismological Commision 1994*. Athens.

Papanikolaou, D. & Danamos, G. 1991. The role of the geotectonic location of Kythira and Cyclades in the geodynamic evolution of the Hellenic Arc. *Bulletin of the Geological Society of Greece*, **25**, 65–79.

Papanikolaou, D. & Royden, L. 2007. Disruption of the Hellenic Arc: Late Miocene extensional detachment faults and steep Pliocene-Quaternary normal faults – or – What happened to Corinth?. *Tectonics*, **26**, TC5003. DOI: 10.1029/2006TC002007.

Papanikolaou, D., Fountoulis, I. & Metaxas, C. 2007. Active faults, deformation rates and Quaternary paleogeography at Kyparissiakos Gulf (SW Greece) deduced from on-shore and off-shore data. *Quaternary International*, **171–172**, 14–30.

Papanikolaou, I. D. 2003. *Generation of high-resolution seismic hazard maps in extensional tectonic settings through integration of earthquake geology, fault mechanics theory and GIS techniques*. PhD thesis, University of London.

Papathanassiou, G. & Pavlides, S. 2007. Using the INQUA scale for the assessment of intensity. Case study on the 2003 Lefkada (Ionian Islands), Greece earthquake. *Quaternary International*, **173–174**, 4–14.

Papazachos, B. C. 1990. Seismicity of the Aegean and surrounding area. *Tectonophysics*, **178**, 287–308.

Papazachos, B. P. & Papazachou, C. B. 1997. *The Earthquakes of Greece*. Ziti Editions, Thessaloniki.

Papazachos, B. C., Comninakis, P. E., Moundrakis, D. M. & Pavlides, S. B. 1982. Preliminary results of an investigation of the February–March 1981 Alkionides Gulf (Greece) earthquakes. *Proceedings of International Symposium on the Hellenic Arc and Trench (H.E.A.T.)*, **2**, 74–87. Q14

Perissoratis, C., Mitropoulos, D. & Angelopoulos, I. 1984. The role of earthquakes in inducing sediments mass movements in the eastern Korinthiakos Gulf. An example from the February 24-March 4, 1981 activity. *Marine Geology*, **55**, 35–45.

Roberts, G. P., Cowie, P., Papanikolaou, I. & Michetti, A. M. 2004. Fault scaling relationships, deformation rates and seismic hazards: An example from the Lazio-Abruzzo Apennines, central Italy. *Journal of Structural Geology*, **26**, 377–398.

Roumelioti, Z., Benetatos, Ch., Kiratzi, A., Stavrakakis, G. & Melis, N. 2004. A study of the 2 December 2002 (M5.5) Vartholomio (western Peloponnese, Greece) earthquake and of its largest aftershocks. *Tectonophysics*, **387**, 65–79.

Serva, L. 1994. Ground effects in the intensity scales. *Terra Nova*, **6**, 414–416.

Serva, L., Esposito, E., Guerrieri, L., Porfido, S., Vittori, E. & Commerci, V. 2007. Environmental effects from five historical earthquakes in southern Apennines (Italy) and macroseismic intensity assessment: Contribution to INQUA EEE Scale project. *Quaternary International*, **173–174**, 30–44.

Stavrakakis, G. N. 1996. Strong motion records and synthetic isoseismals of the Pyrgos, Peloponnisos, southern Greece, earthquake sequence of March 26, 1993. *Pure and Applied Geophysics*, **146**, 147–161.

Tatevosian, R. E. 2007. The Verny, 1887, earthquake in Central Asia: Application of the INQUA scale, based on coseismic environmental effects. *Quaternary International*, **173–174**, 23–29.

Taymaz, T., Jackson, J. & McKenzie, D. 1991. Active tectonics of the north and central Aegean Sea. *Geophysical Journal International*, **106**, 433–490.

Tilford, N. R., Chandra, U., Amick, D. C., Moran, R. & Snider, F. 1985. Attenuation of the intensities and effect of local site conditions on observed intensities during the Corinth, Greece, Earthquake of 24 and 25 February and 4 March 1981. *Bulletin of the Seismological Society of America*, **75**, 923–937.